2015

Predicting Carbon Isotope Discrimination in Eelgrass (Zostera marina L.) From the Environmental Parameters- Light, Flow, and [DIC]

Meredith L. McPherson

Richard C. Zimmerman
Old Dominion University, rzimmerm@odu.edu

Victoria J. Hill
Old Dominion University

Original Publication Citation

McPherson, M.L., Zimmerman, R.C., & Hill, V.J. (2015). Predicting carbon isotope discrimination in eelgrass (*Zostera marina* l.) from the environmental parameters light, flow, and dic. *Limnology and Oceanography, 60*(6), 1875-1889. doi: 10.1002/lno.10142

LIMNOLOGY
and
OCEANOGRAPHY

ASLO

Limnol. Oceanogr. 60, 2015, 1875–1889

doi: 10.1002/lno.10142

Predicting carbon isotope discrimination in Eelgrass (*Zostera marina* L.) from the environmental parameters—light, flow, and [DIC]

Meredith L. McPherson,[a]* Richard C. Zimmerman, Victoria. J. Hill
Department of Ocean, Earth & Atmospheric Sciences, Old Dominion University, Norfolk, Virginia

Abstract

Isotopic discrimination against ^{13}C during photosynthesis is determined by a combination of environmental conditions and physiological mechanisms that control delivery of CO_2 to RUBISCO. This study investigated the effects of light, flow, dissolved inorganic carbon (DIC) concentration, and its speciation, on photosynthetic carbon assimilation of *Zostera marina* L. (eelgrass) using a combination of laboratory experiments and theoretical calculations leading to a mechanistic understanding of environmental conditions that influence leaf carbon uptake and determine leaf stable carbon isotope signatures ($\delta^{13}C$). Photosynthesis was saturated with respect to flow at low velocity ($\sim$ 3 cm s^{-1}), but was strongly influenced by [DIC], and particularly aqueous CO_2 ($CO_{2(aq)}$) under all flow conditions. The non-linear responses of light- and flow-saturated photosynthesis to [DIC] were used to quantify the maximum physiological capacity for photosynthesis, and to determine the degree of photosynthetic carbon limitation for light-saturated photosynthesis, which provided a mechanistic pathway for modeling regulation of carbon uptake and ^{13}C discrimination. Model predictions of $\delta^{13}C$ spanned the typical range of values reported for a variety of seagrass taxa, and were most sensitive to [DIC] (predominantly [$CO_{2(aq)}$]) and flow, but less sensitive to DIC source [$CO_{2(aq)}$ vs. HCO_3^-]. These results provide a predictive understanding of the role of key environmental parameters (light, flow, and DIC availability) can have in driving $\delta^{13}C$ of seagrasses, which will become increasingly important for predicting the response of these ecosystem engineers to local processes that affect light availability and flow, as well as global impacts of climate warming and ocean acidification in the Anthropocene.

Isotopic discrimination against ^{13}C during photosynthetic carbon assimilation results from both plant metabolic processes and environmental conditions (O'Leary 1981). Variations in isotopic composition ($\delta^{13}C$) of terrestrial plants are often attributed to taxon-specific metabolic pathways for carbon acquisition that make terrestrial C_3 plants isotopically lighter (−35‰ to −20‰) than their C_4 counterparts (−15‰ to −9‰) (Smith and Epstein 1971). Unlike terrestrial photosynthesis, which depends solely on atmospheric CO_2, aquatic photosynthesis can be driven by two sources of dissolved inorganic carbon (DIC)—dissolved aqueous CO_2 [$CO_{2(aq)}$] and bicarbonate (HCO_3^-). Although $CO_{2(aq)}$ is readily used by all aquatic photoautotrophs, the low concentrations (10–15 μmol L^{-1}) present in air-saturated seawater are typically insufficient to satisfy photosynthetic demand in high light environments. The photosynthetic limitations imposed by low [$CO_{2(aq)}$] are overcome in most aquatic plants (marine algae and some vascular plants) by carbon concentrating mechanisms (CCM) that exploit HCO_3^- (Madsen and Sand-Jensen 1991), concentrations of which can exceed 2 mM in seawater. Since HCO_3^- and $CO_{2(aq)}$ have characteristically different stable carbon isotope signatures in seawater ($\delta^{13}C \approx 0$‰ vs. −9‰, respectively), their differential utilization may also influence isotopic discrimination during carbon assimilation (Raven et al. 2002).

Seagrasses, a polyphyletic group of aquatic C_3 angiosperms, have isotopic signatures that are much heavier than terrestrial C_3 angiosperms (Peterson and Fry 1987) and most of their aquatic macroalgal counterparts. Although $\delta^{13}C$ signatures of seagrass taxa range from −23‰ to −3‰ (Hemminga and Mateo 1996), they are typically heavier ($\approx$ −10‰) than values reported for marine phytoplankton ($\approx$ −24‰; France 1995) and marine macroalgae (−20‰ to −15‰; Raven et al. 1995). The capacity to dehydrate/transport HCO_3^- for photosynthesis differs among seagrasses and other marine autotrophs, and may be responsible for some of the observed variation in $\delta^{13}C$ signature (Hemminga and Mateo 1996).

Within individual seagrass taxa, the carbon isotope signature can be influenced by a variety of environmental and

*Correspondence: mmcpher1@ucsc.edu
[a]Present address: Department of Ocean Sciences, University of California Santa Cruz, Santa Cruz, California

physiological conditions including: (1) the source and concentration of inorganic carbon (Hemminga and Mateo 1996; James and Larkum 1996; Raven et al. 2002); (2) water temperature altering the solubility of $CO_{2(aq)}$ in seawater (Zhang et al. 1995); (3) viscous boundary layers affecting diffusion of $CO_{2(aq)}$ across the leaf-water interface (Smith and Walker 1980; Hurd 2000); and (4) internal carbon concentrating mechanisms, such as recycling of CO_2 in the lacunae (Grice et al. 1996). Light availability influences photosynthetic carbon uptake, and several studies inferred a significant positive relationship between seagrass $\delta^{13}C$ and light/photosynthesis from the commonly reported negative correlation between seagrass $\delta^{13}C$ and depth (Cooper and Deniro 1989; Grice et al. 1996; Campbell and Fourqurean 2009), as well as seasonal cycles in $\delta^{13}C$ values (Fourqurean et al. 2005; Kim et al. 2014). The impact of light availability on seagrass $\delta^{13}C$ was recently placed on a stronger theoretical foundation by showing that the $\delta^{13}C$ signature of *Thalassia testudinum* leaves was related to the daily period of irradiance saturated photosynthesis when carbon limitation of photosynthesis reduces the ability of RUBISCO to discriminate against $^{13}CO_2$ (Hu et al. 2012).

In addition to carbon sources and light availability, important physical and physiological conditions control the permeability of inorganic carbon through the external fluid boundary layer plus internal leaf structures that create a physical barrier between the water and the chloroplast stroma (Smith and Walker 1980). Water motion increases permeability by reducing the thickness of the unstirred boundary layer around the leaf, regardless of whether the bulk flow is laminar or turbulent (Denny 1993; Hurd 2000). Permeability is also affected by temperature, salinity, and alkalinity which combine to control the chemical speciation of DIC into $CO_{2(aq)}$, HCO_3^-, and CO_3^{2-}, and the diffusion coefficients of these carbon species in seawater (Zeebe and Wolf-Gladrow 2001).

Marine angiosperms must overcome many physiological and environmental challenges to survive. High light requirements, driven by high physiological demands for dissolved $CO_{2(aq)}$ (Invers et al. 2001; Palacios and Zimmerman 2007), make seagrasses particularly vulnerable to anthropogenic stress (Orth et al. 2006). In addition to stimulating seagrass productivity, the increased availability of DIC, and particularly $CO_{2(aq)}$, associated with ocean acidification may facilitate isotopic discrimination aginst $^{13}CO_2$ as it stimulates leaf photosynthesis (Duarte 2002; Palacios and Zimmerman 2007; Jiang et al. 2010) thereby decreasing the $\delta^{13}C$ isotopic signature of seagrass leaves in an acidified ocean.

The objective of this study was to investigate the effects of water flow, DIC concentration and speciation [$CO_{2(aq)}$ vs. HCO_3^-] on photosynthetic carbon uptake rates and assimilation using a mathematical model parameterized by laboratory experiments in order to develop a predictive understanding of the impacts of substrate availability on carbon isotope fractionation by *Zostera marina* L. (eelgrass), the most abundant species of seagrass in temperate waters of the northern hemisphere. By increasing our mechanistic understanding of the environmental regulation of photosynthesis in seagrasses, this model can facilitate our understanding of the relationship between the environment and natural variation in $\delta^{13}C$ in seagrass populations that may help predict the response of seagrasses to a changing marine climate.

Methods

Theoretical development

Photosynthetic isotope discrimination in terrestrial plants is strongly influenced by stomatal conductance that regulates the diffusion of CO_2 from the fluid (air) boundary to the photosynthetic cells in the leaf mesophyll, as well as the enzymatic fractionation associated with RUBISCO (Farquhar et al. 1989). Aquatic photosynthesis, however, occurs in unicellular algae, and epidermal cell layers of seagrass leaves and macroalgal thalli, all of which lack stomata. In the absence of stomatal regulation of CO_2 diffusion, the general models developed for isotopic discrimination in terrestrial plants collapse to the enzymatic fractionation associated with RUBISCO. However, the slow diffusion rate of $CO_{2(aq)}$ through water relative to air, combined with its relatively low concentration and interchangeability with HCO_3^-, requires a different approach to modeling isotopic fractionation in aquatic autotrophs. Table 1 provides a list of all symbols, their definitions and units used in developing the model outlined below.

The non-linear relationship between light availability and photosynthesis (P) in seagrass is well approximated by the negative exponential function originally developed by Poisson from target theory, and pioneered for photosynthesis by Webb et al. (1974):

$$P = P_E \times (1 - e^{-E_d/E_k}) \quad (1)$$

where E_d is the downwelling plane irradiance incident on the leaf surface, E_k is the plane irradiance required to saturate photosynthesis, and P_E is the light-saturated rate of photosynthesis. In this light-dependent model, P approaches P_E as E_d approaches E_k, where $E_k = P_E/\alpha$, and α is the slope of the light limited region of the P vs. E_d curve.

Most production models treat P_E as the physiological maximum rate of photosynthesis (often denoted as P_m), at least with respect to external environmental influences. However, because light-saturated photosynthesis of eelgrass (and most seagrasses) is carbon-limited in natural seawater, P_E is considered here as a variable term that depends on the delivery of CO_2 to the reaction site of carbon fixation, the control of which can be expressed as a square root quadratic (hyperbolic) function of substrate concentration and permeability (Hill and Whittingham 1955; Smith and Walker 1980):

Table 1. Summary of symbols, their definitions, and dimensions.

Symbol	Definition	Dimensions	Literature published value	Source
Basic parameters				
DIC	Dissolved inorganic carbon			
A_T	Total alkalinity	mEq L^{-1}		
d*C*/d*t*	Measured eelgrass carbon uptake	μmol C m^{-2} s^{-1}		
$\delta^{13}C$	Isotopic ratio for carbon	‰		
E_d	Downwelling plane irradiance	μmol quanta m^{-2} s^{-1}		
E_k	Saturation plane irradiance	μmol quanta m^{-2} s^{-1}		
Photosynthetic parameters				
α	Slope of the light-limited region of *P* vs. *E* curve	μmol C m^{-2} min^{-1}/μmol quanta m^{-2} s^{-1}	3.1	Zimmerman et al. (1997); assumes $1CO_2$:$1O_2$
β	Slope of the flow-limited region of the U_P vs. *u*	μmol C m^{-2} s^{-1}/m s^{-1}		
P	Realized light-limited photosynthetic rate	μmol C m^{-2} s^{-1}		
P_m	Physiological maximum photosynthetic rate	μmol C m^{-2} s^{-1}		
Hill-Whittingham (1955) parameters				
c	Mainstream [DIC] or $[CO_{2(aq)}]$	μmol L^{-1}		
K_s	Concentration of substrate (CO_2) at ½ P_m	μmol L^{-1}		
P_E	Light-saturated photosynthesis	μmol C m^{-2} s^{-1}		
P_F	Light- and flow-saturated photosynthesis	μmol C m^{-2} s^{-1}		
u	Laminar flow velocity	cm s^{-1}		
U_p	Permeability of the unstirred layer	μm s^{-1}		
U_{pF}	Flow-saturated permeability of the unstirred layer	μm s^{-1}		
U_{p0}	Diffusive permeability under light-saturated conditions	μm s^{-1}		

$$P_E = \frac{1}{2}\{(K_s U_p + cU_p + P_F) - [(K_s U_p + cU_p + P_F)^2 - 4cU_p P_F]^{\frac{1}{2}}\} \quad (2)$$

Here, *c* represents the inorganic carbon concentration of the mainstream water and P_F represents the rate of carbon-limited photosynthesis under light and flow saturation empirically described by the Monod equation:

$$P_F = P_m \frac{[DIC]}{K_s + [DIC]} \quad (3)$$

where K_s is the empirical half-saturation constant based on external [DIC] under flow saturation, and P_m represents the maximum physiological capacity for photosynthesis under light, flow, and DIC saturation. The effect of [DIC] on P_F can be expanded to account for the separate effects of $CO_{2(aq)}$ and HCO_3^-:

$$P_F = P_{m(CO_{2(aq)})} \frac{[CO_{2(aq)}]}{K_{s(CO_{2(aq)})} + [CO_{2(aq)}]} + P_{m(HCO_3^-)} \frac{[HCO_3^-]}{K_{s(HCO_3^-)} + [HCO_3^-]} \quad (3a)$$

U_p controls the permeability of DIC through an unstirred fluid boundary of variable thickness controlled by flow, plus all the structural leaf elements (cell membranes, etc.) that resist the diffusion from the leaf surface to the reaction site in the stroma of the chloroplast. For a given concentration (*c*) of DIC in the bulk fluid, flow exerts a saturation type response on U_p that can be expressed using a negative exponential function similar in form to Eq. 1:

$$U_p = U_{pF} \times [1 - e^{-(\beta \cdot u / U_{pF})}] + U_{p0} \quad (4)$$

where *u* represents the laminar velocity of the bulk fluid outside the boundary layer and β is the slope of the flow-limiting region of the U_p vs. *u* curve. U_{p0} represents the diffusive permeability of DIC across the leaf surface under light-saturated conditions in stagnant water (i.e., when $u = 0$).

The $\delta^{13}C$ signature was modeled as a negative linear relationship between the degree of isotopic fractionation by RUBISCO, and the ratio of P_E/P_m derived from Eqs. 1–4 that quantified the degree to which light-saturated photosynthesis was carbon-limited by external conditions (i.e., [DIC] and/or flow). When light was limiting or P_E was carbon- and flow-saturated (i.e., $P < P_E$ or $P_E/P_m = 1$), RUBISCO was not carbon-limited and assimilation fractionated against $^{13}CO_2$ at −28‰ relative to the DIC source, based on the inherent fraction capacity of RUBISCO (Falkowski and Raven 2007). When *P* was light-saturated (i.e., $P = P_E$), but limited by flow or DIC concentration (i.e., $P_E/P_m < 1$), leaf $\delta^{13}C$ was

isotopically heavier, or less negative, because RUBISCO discriminated less against $^{13}CO_2$. The absolute capacity for RUBISCO to discriminate against $^{13}CO_2$ was also influenced by $\delta^{13}C$ of the DIC source, which was derived from the combined $\delta^{13}C$ signatures of HCO_3^- ($\delta^{13}C = 0‰$) and $CO_{2(aq)}$ ($\delta^{13}C = -9‰$; Kroopnick 1985) available to the plant, nominally based on source water alkalinity and pH.

Model parameterization

The physiological terms required to parameterize Eqs. 1 through 4 [P_E, P_F, U_p, U_{pF}, and U_{p0}] were quantified using laboratory measurements of ^{14}C uptake using individual leaves of eelgrass collected from the Chesapeake Bay National Estuarine Research Reserve site at the Goodwin Islands (CBNERR-GI, 37° 13′ N; 76° 23′ W), near the mouth of the York River in Chesapeake Bay, Virginia, and from literature values (Table 1). Parameterization of P_m and K_s for intact leaves for flow-saturated conditions over a range of [DIC] was determined using the non-linear curve-fitting tool implemented in MATLAB® (R2012b).

Whole eelgrass shoots were collected for laboratory experiments on 15 August 2011, 08 February 2012, 06 June 2012, and 14 July 2012. Approximately 100 shoots were transplanted into plastic trays filled with sediment obtained from the Goodwin Islands collection site and placed in a 60 L plastic aquaria filled with artificial seawater made from Instant Ocean® Sea Salt to a salinity of 18 PSU to mimic salinity conditions of CBNERR-GI. Tanks were maintained inside a greenhouse for not more than 1 week prior to use in the experiments described below. During that time, irradiance was supplied by the natural diurnal cycle of sunlight filtered through translucent plastic panels (60% PAR transmission, UV opaque). The aquarium was kept at room temperature (20–25°C) and aerated with aquarium pumps to provide mixing and avoid boundary-layer limitation of leaf metabolic processes that might result from a stagnant water column.

Light-saturated uptake of ^{14}C (P_E) was measured using the second youngest leaves determined by the order in which leaves emerge from the sheath; the inner-most leaf was the youngest. All measurements were performed at 25°C at flow velocities of 0 ($n = 13$); 1 ($n = 7$); 2 ($n = 7$); 3 ($n = 2$); 3.5 ($n = 2$); 4 ($n = 2$); and 15 ($n = 9$) cm s^{-1} in a recirculating 1.7 L flume chamber (30 × 6 × 5 cm) constructed of clear polycarbonate equipped with a variable speed inline pump. Varying measurement replication for each flow rate was not a result of experimental failures, but rather the evolution of the procedure over the course of the research. The incubation medium consisted of 0.45 μm filtered, air-saturated water collected from the CBNERR-GI field site, (salinity = 18 to 20 PSU, alkalinity = ~ 1700 mEq kg^{-1}, [DIC] = ~ 1500 μmol L^{-1}). All incubations were performed by placing a leaf in the center of the working section for 15 min. Photosynthesis-saturating irradiance (~ 250 μmol quanta m^{-2} s^{-1}) was provided by a 300 W quartz halogen lamp placed directly above the leaf. Unidirectional laminar flow within the working section was produced by forcing the water through aeronautical honeycombs (Plascore, Direct Industry) placed at both ends of the flume. Flow conditions were not perfectly laminar at the highest flume velocity (15 cm s^{-1}), but this was well beyond the threshold for flow saturation of DIC uptake. Temperature was separately regulated by a thermostatically controlled circulating water bath system jacketing the recirculating tube and connected to an aluminium cooling plate positioned directly under the working section.

Separate incubations were conducted in the presence of 75 μmol L^{-1} acetazolamide (AZ), an inhibitor of carbonic anhydrase activity (Bjork et al. 1997; Hellblom and Björk 1999; Invers et al. 1999) at flows of 0 ($n = 5$), 1 ($n = 6$), 2 ($n = 6$), and 15 ($n = 6$) cm s^{-1} to estimate the degree of HCO_3^- utilization. Prior to running experiments, AZ activity was verified by measuring the reduction of pure CA enzyme activity in buffer solution similar to control experiments conducted by Mercado et al. (2003). Water in the flume was inoculated with 5 mL of 25 mmol L^{-1} AZ stock solution prepared in 0.05 M NaOH, which increased the alkalinity of the incubation medium by 173 μEq kg^{-1}, and altered the concentrations of $CO_{2(aq)}$, HCO_3^- and CO_3^{2-} by −35.5% (−4.3 μmol L^{-1}), +1.83% (26.2 μmol L^{-1}), and +61.4% (63.0 μmol L^{-1}), respectively. Differences in photosynthesis between AZ and non-AZ flume runs were evaluated using Student's *t*-test.

The effect of [DIC] on light- and flow-saturated photosynthesis was measured by ^{14}C uptake using a magnetically stirred, sealed water-jacketed glass chamber rather than the flume, because it was simpler to seal the small (5 mL) chamber without trapping gas bubbles in the system and manipulate the total [DIC] without losing $^{14}CO_2$ to the atmosphere at low pH. [DIC] in the chamber was manipulated by bubbling with compressed CO_2 to a range of predetermined pH values (6–8) prior to introducing ^{14}C and sealing the chamber. The speciation of DIC into $CO_{2(aq)}$, HCO_3^- and CO_3^{2-} for each treatment was calculated using CO2SYS (Ver. 1.05; Lewis and Wallace 2006), based on the salinity, alkalinity, and temperature of the incubation water. Saturating flow in the small chamber, typically used to measure O_2 flux, was provided by a magnetic stirrer that created a turbulent environment and prevented boundary layer limitation of DIC substrates to the leaf.

Aliquots of 50 μCi L^{-1} and 0.025 μCi L^{-1} of $NaH^{14}CO_3$ (PerkinElmer) were added immediately prior to all incubations in the flume and 5 mL chamber, respectively. The solutions were circulated for a minimum of 10 min before introducing leaves to the chambers. Control incubations performed using the unsealed flume without leaf segments showed no measurable loss of ^{14}C from the water by volatilization across the open air–water interface during the incubation period. The 5 mL chamber was sealed immediately after

introducing the $NaH^{14}CO_3$, and opened briefly (< 30 s) after 10 min to introduce the leaf segment, and then resealed to prevent measurable loss of $^{14}CO_2$, even at low pH. At the end of each incubation, leaves were washed for 2 min in CBNERR-GI water containing 10% (v/v) HCl to remove unincorporated ^{14}C from the external surfaces, then ground in NCS® tissue solubilizer using a glass homogenizer and transferred to 20 mL glass vials containing scintillation cocktail (Fisher Scientific Scintiverse™ BD Cocktail 5X18-4). Radioactivity was counted using a Beckman liquid scintillation counter (LS 5000TD). Disintegrations per minute (dpm) were corrected for quenching using internal standardization and verified across a range of standard ^{14}C activities in NCS®-leaf homogenate solution prior to experimental runs. Counts of ^{14}C standards added to non-radioactive leaf homogenates in NCS® showed no measurable interference (i.e., self-quenching) from leaf pigments or other materials in the tissue homogenates.

Carbon uptake rates were determined from the ratio of ^{14}C incorporated into the leaves (dpm_{sample}) to the total ^{14}C in the incubation medium (dpm_{added}), according to Penhale (1977):

$$P = \frac{\mathrm{dpm}_{\mathrm{sample}} \times [\mathrm{DIC}]}{A \times \mathrm{dpm}_{\mathrm{added}} \times t} \quad (5)$$

where [DIC] was the total dissolved inorganic carbon in the water (after isotopic addition), A was the one-sided area (m^2) of the incubated leaf sample, and t was the incubation time. No correction for isotopic discrimination against ^{14}C during photosynthesis was applied to carbon uptake calculations as the effect was smaller than the precision of our measurements. U_p ($\mu m\ s^{-1}$) was calculated as the leaf area-specific rate of DIC uptake (dC/dt) normalized to the bulk [DIC], which was assumed equivalent to the concentration gradient (dc) between the external bulk fluid and the reaction site of RUBISCO when photosynthesis was carbon limited:

$$U_p = \frac{dC/dt}{[\mathrm{DIC}]} \quad (6)$$

Although the true gradient (dc) is probably < [DIC], the increase in U_p resulting from a decrease in the denominator of Eq. 6 based on the true gradient is offset by compensating changes in the value of K_s in Eqs. 2 and 3. Thus, uncertainty in the true value of the gradient, which is very difficult to quantify, did not affect determination of P_F (Eq. 3), P_E (Eq. 2) or, ultimately, $\delta^{13}C$ by the model.

Concentrations of $CO_{2(aq)}$, HCO_3^- and total DIC were determined by CO2SYS Ver. 1.05 (Lewis and Wallace 2006) using the NBS buffer scale from measured values of temperature, salinity, pH, and total alkalinity (TA). Salinity was measured using a refractometer calibrated with deionized water. Incubation medium pH was measured using a Cole Parmer pH/mV/°C meter (Model # 59003-00) and epoxy-body general purpose electrode calibrated with NBS buffers using a three point buffer system (Oakton). Alkalinity titrations were conducted prior to each photosynthesis experiment according to Gieskes and Rogers (1973) using 0.02N HCl (Fisher Certified 0.0198 to 0.0202N).

Light- and flow-saturated photosynthesis data across a pH range (6–9) measured under constant [DIC] but varying [$CO_{2(aq)}$] for four species of seagrass (*Posidonia oceanica* L., *Zostera marina*, *Phyllospadix torreyi*, and *Cymodocea nodosa*) were extracted from Fig. 2 of Invers et al. (2001) and combined with the kinetic estimates for [HCO_3^-] provided in their Table 4 to determine the relative contribution of $CO_{2(aq)}$ and HCO_3^- to photosynthesis as a function of [DIC], and calculate P_E/P_m for [HCO_3^-], [$CO_{2(aq)}$], and [$HCO_3^- + CO_{2(aq)}$] to predict $\delta^{13}C$ for light-saturated photosynthesis. Similar to above, predictions of P_F, P_m and K_s for each respective substrate were individually adjusted for each seagrass species using the curve-fitting tool in MATLAB® (R2012b). Resulting $\delta^{13}C$ were compared to genus-specific $\delta^{13}C$ ranges reported by Hemminga and Mateo (1996, their Table 1).

Results

Model parameterization

Permeability (U_p) calculated from ^{14}C uptake rates (Eq. 6) showed a saturation-type response to flow that was well approximated by a negative exponential function (Eq. 4), whether the bulk concentration of inorganic carbon substrate (c) was assumed to be $CO_{2(aq)}$ ($\sim 10\ \mu mol\ L^{-1}$) or the total DIC pool ($\sim 2000\ \mu mol\ L^{-1}$; Fig. 1A, $r^2 = 0.989$ and 0.996, respectively). U_{pCO2} calculated using $CO_{2(aq)}$ increased linearly as a function of flow (slope = 45.4×10^{-4}) to a saturation value of $101 \pm 4.2\ \mu m\ s^{-1}$ at a flow rate of $2.2 \pm 0.05\ cm\ s^{-1}$. The initial slope (β) for U_p calculated using total DIC (U_{pDIC}) was markedly less steep (slope = 0.2×10^{-4}) than U_{pCO2}. Additionally, flow saturation occurred at $4.5 \pm 0.2\ cm\ s^{-1}$ and maximum U_{pDIC} ($0.9 \pm 0.1\ \mu m\ s^{-1}$) was 112 times lower than the maximum U_{pCO2}. The flow dependent parameterization of U_{pDIC} characterized P_E accurately using Eq. 2 across the range of flows measured in the flume (Fig. 1B, symbols) using total DIC as the substrate (c), and setting our empirical K_s to the Michaelis–Menten dissociation constant for RUBISCO ($K_m \cong 12\ \mu mol\ L^{-1}$; $r^2 = 0.676$). However, when the flow dependent parameterization of U_p was based on $CO_{2(aq)}$ (i.e., $c = [CO_{2(aq)}]$), holding K_s at $12\ \mu mol\ L^{-1}$ caused Eq. 2 to underestimate P_E by a factor of 3 (Fig. 1B). Relaxing the constraint on K_s from 12 $\mu mol\ L^{-1}$ allowed Eq. 2 to accurately predict light- and flow-saturated photosynthesis (P_F; Fig. 2A; Table 2), but the resulting values for K_s were 194 $\mu mol\ L^{-1}$ $CO_{2(aq)}$ (Fig. 2A; Table 2) and 1500 $\mu mol\ L^{-1}$ DIC (Fig. 2B; Table 2), both higher than K_m for RUBISCO. P_E exhibited a saturation type

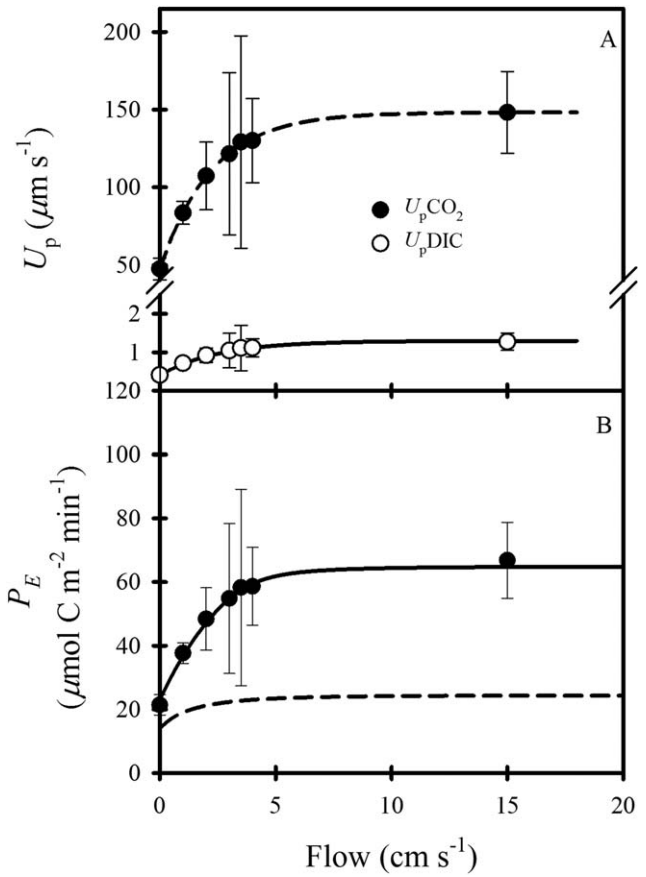

Fig. 1. (A) Effect of flow on permeability of the unstirred layer based on bulk [DIC] (U_{pDIC}; open symbols), and [$CO_{2(aq)}$] (U_{pCO2}; filled symbols). The curves represent non-linear least squares fits to Eq. 6. $r^2 = 0.989$ and 0.996, for U_{pDIC} (solid line) and U_{pCO2} (dashed line), respectively. Error bars indicate ± 1 standard error of the mean ($n = 36$). (B) Measured light-saturated photosynthesis (P_E; symbols, ± 1 SE, $n = 36$) without acetazolamide (AZ). Modeled photosynthesis without AZ, for $K_s = 12$ μM (Falkowski and Raven 2007) calculated from total [DIC] (solid line; $r^2 = 0.676$) and [$CO_{2(aq)}$] (dashed line) using Eq. 2, plotted as a function of flow.

response to flow (Fig. 1B) and in stagnant water (0 flow) was reduced to about 1/3 of the flow-saturated value. Acetazolamide did not significantly inhibit photosynthesis at flow rates of 0 cm s^{-1}, 1 cm s^{-1}, and 15 cm s^{-1}, and actually appeared to enhance photosynthesis at 2 cm s^{-1} (Table 3).

Non-linear fits of light- and flow-saturated photosynthesis (P_F) to $CO_{2(aq)}$ and DIC using Eqs. 2 and 3 showed similar saturation type responses to decreased pH (Fig. 2A,B; Table 2) resulting primarily from the 150-fold increase in [$CO_{2(aq)}$] (Fig. 2C). In contrast, [HCO_3^-] remained relatively constant from pH 6 to 8 (Fig. 2C). At 2534 μmol L^{-1} DIC (pH 6), 92% of DIC was [$CO_{2(aq)}$] vs. only 0.01% at 1058 μmol L^{-1} (pH 8.0). Regardless of the presumed substrate, the model revealed that photosynthesis approached 0 when [$CO_{2(aq)}$] dropped below 3.1 μmol L^{-1} (pH = 8.51; Fig. 2A). Furthermore, the calculated K_s values of 1500 and 194 μmol L^{-1} for

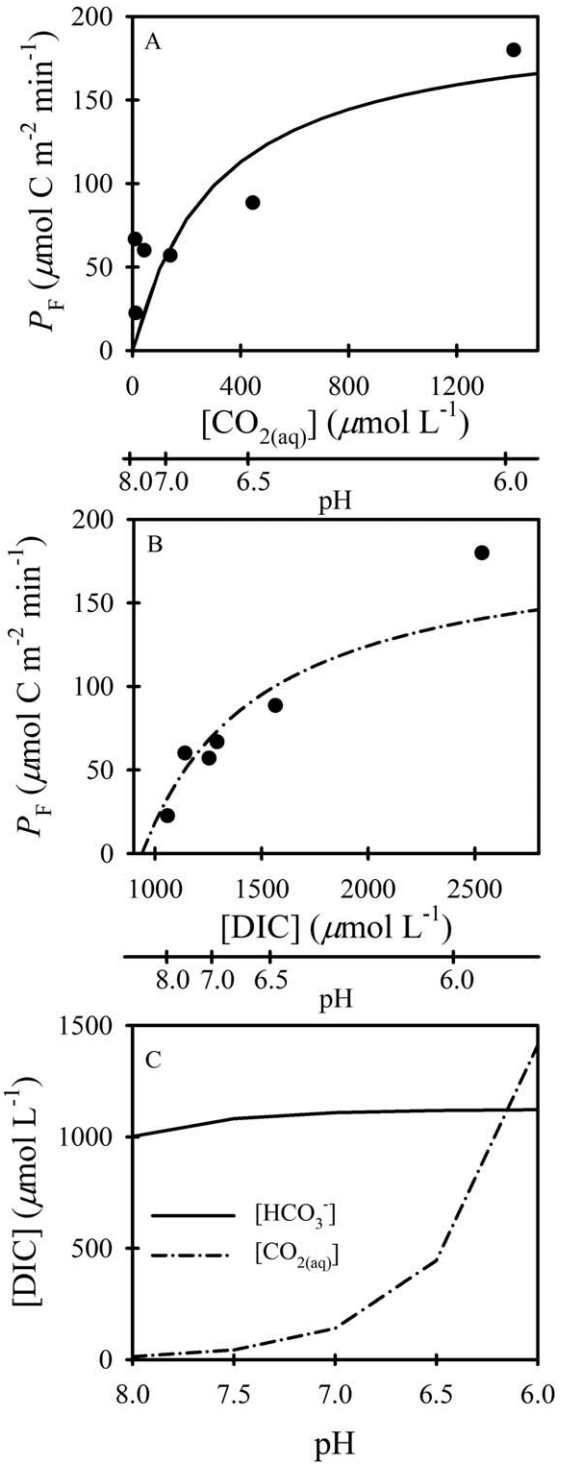

Fig. 2. (A) Measured light- and flow-saturated photosynthesis plotted as a function of [$CO_{2(aq)}$] and pH fitted to Eqs. 2–4. (B) Measured light- and flow-saturated photosynthesis plotted as a function of bulk [DIC] and pH fitted to Eqs. 2–4 using a positive *x*-intercept such that photosynthesis = 0 at 940 μM DIC [= 3.1 μM $CO_{2(aq)}$]. Parameter values and their error estimates for curves shown in A and B are provided in Table 2. (C) Concentration of HCO_3^- and $CO_{2(aq)}$ as a function of pH for experimental seawater alkalinity conditions.

Table 2. Model parameter values generated by non-linear curve fits to the experimental data using Eqs. 2–4, their respective units, and statistics for DIC vs. flow–saturated photosynthesis (P_F) and $CO_{2(aq)}$ vs. P_F curves (Fig. 2A,B). K_s is the half-saturation constant for the dependence of P_F on $[CO_{2(aq)}]$ (Eq. 3), P_m is the maximum physiological capacity for photosynthesis (Eq. 3), U_{pF} is the flow-saturated permeability of the unstirred layer (Eq. 4). R^2 is the adjusted non-linear regression coefficient of determination.

	Units	DIC vs. P_F	$CO_{2(aq)}$ vs. P_F
K_s	μmol L^{-1}	1499 ± 293	194 ± 357
P_m	μmol C m^{-2} min^{-1}	190 (fixed)	174 ± 147
U_{pF}	μm s^{-1}	5 ± 250	118 ± 845
x-intercept	μmol L^{-1}	940 ± 233	0 ± 0
Equivalent pH at $P = 0$		8.51	9.23
R^2		0.86	0.67

both DIC and $CO_{2(aq)}$, respectively, were well above the published K_m values for RUBISCO (Table 2). Reported mean U_{pF} values based on $CO_{2(aq)}$ and DIC were 118 μm s^{-1} and 5 μm s^{-1}, respectively (Table 2). However, standard errors were large (845 μm s^{-1} and 250 μm s^{-1}, respectively), and the means were not significantly different from each other or from zero.

Although permeability (U_p) depends on both substrate concentration (Eq. 6) and flow (Eq. 4), flow exerted the dominant influence on U_p at DIC > 1000 μmol L^{-1} (Fig. 3A). Further, U_p was relatively insensitive to increases in [DIC] up to 2534 μmol L^{-1}, but light-saturated photosynthesis (P_E) was strongly influenced by [DIC] under all flow conditions as the linear slope for flow-limited photosynthesis increased fourfold between DIC concentrations of 1058 μmol L^{-1} and 2534 μmol L^{-1} (Fig. 3B).

Flow and DIC concentration combined to influence photosynthesis-irradiance responses (Fig. 4). By definition, photosynthesis for all DIC conditions was 0 across all flows in the dark ($E_d = 0$). For both 0 flow and flow-saturated conditions, the threshold for irradiance saturation responded positively to external $[CO_{2(aq)}]$ across all four DIC treatments

Table 3. Results of Student's *t*-test comparing photosynthesis measurements at specific flows for flume runs with and without acetacolamide (AZ). Error estimates represent standard errors.

Flume flow (cm s^{-1})	*t*-value	df	*p*-value	P_E (No AZ)	P_E (AZ)
0	1.5	16	0.08	21 ± 12	42 ± 20
1	0.97	11	0.17	38 ± 9	48 ± 15
2	2.4	11	0.02	48 ± 42	106 ± 9
15	0.8	13	0.22	67 ± 36	98 ± 50

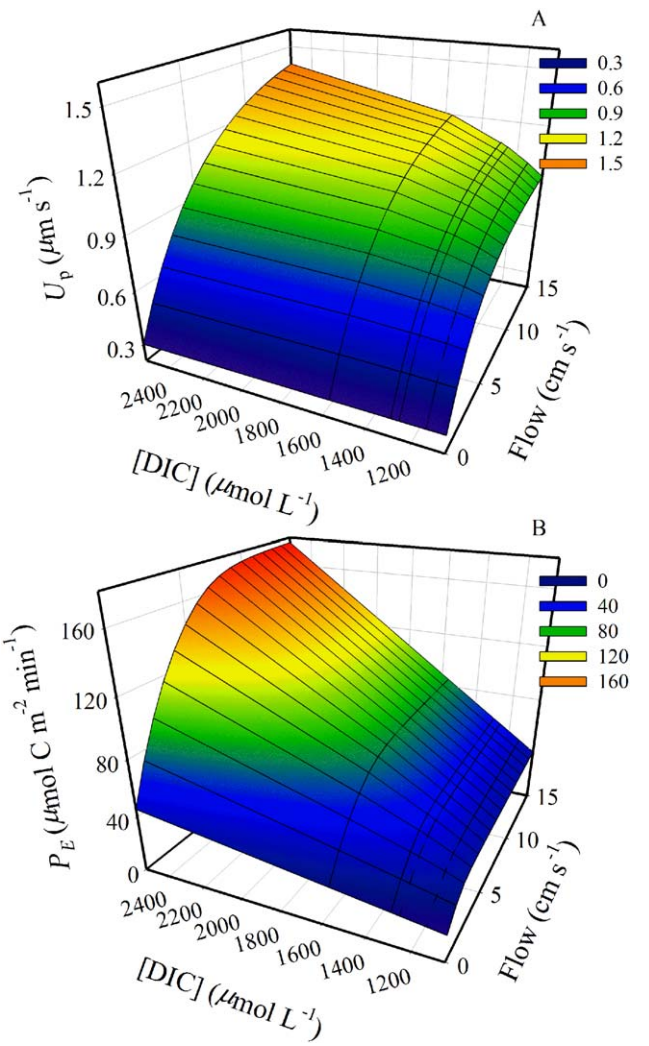

Fig. 3. (A) Combined effects of [DIC] and flow (Eq. 6) on permeability (U_p). (B) Combined effects of [DIC] and flow on light-saturated photosynthesis (P_E; Eq. 2). [Color figure can be viewed in the online issue, which is available at wileyonlinelibrary.com.]

(Fig. 4; Table 4). Under flow saturation, increases in $[CO_{2(aq)}]$ increased E_k 4.6-fold (Fig. 4A,D; $E_k = 13$ μmol quanta m^{-2} s^{-1} and 60 μmol quanta m^{-2} s^{-1}, respectively), but the increase was only 2.5-fold in still water (Fig. 4A,D; $E_k = 6$ μmol quanta m^{-2} s^{-1} and 15 μmol quanta m^{-2} s^{-1}). For constant DIC, the irradiance required to saturate photosynthesis (E_k) also increased with flow as the boundary layer became more permeable to DIC, reducing the degree of carbon limitation. Similar to shifts in light saturation, flow saturation increased as a function of [DIC] and ranged from 3 cm s^{-1} to 11 cm s^{-1} between 1058 μmol L^{-1} to 2534 μmol L^{-1} DIC (Fig. 4A,D). This ability to model the combined effects of light, flow, and [DIC] on eelgrass photosynthesis provided the endmember values and a mechanistic pathway for modeling the environmental regulation of carbon uptake and isotope partitioning.

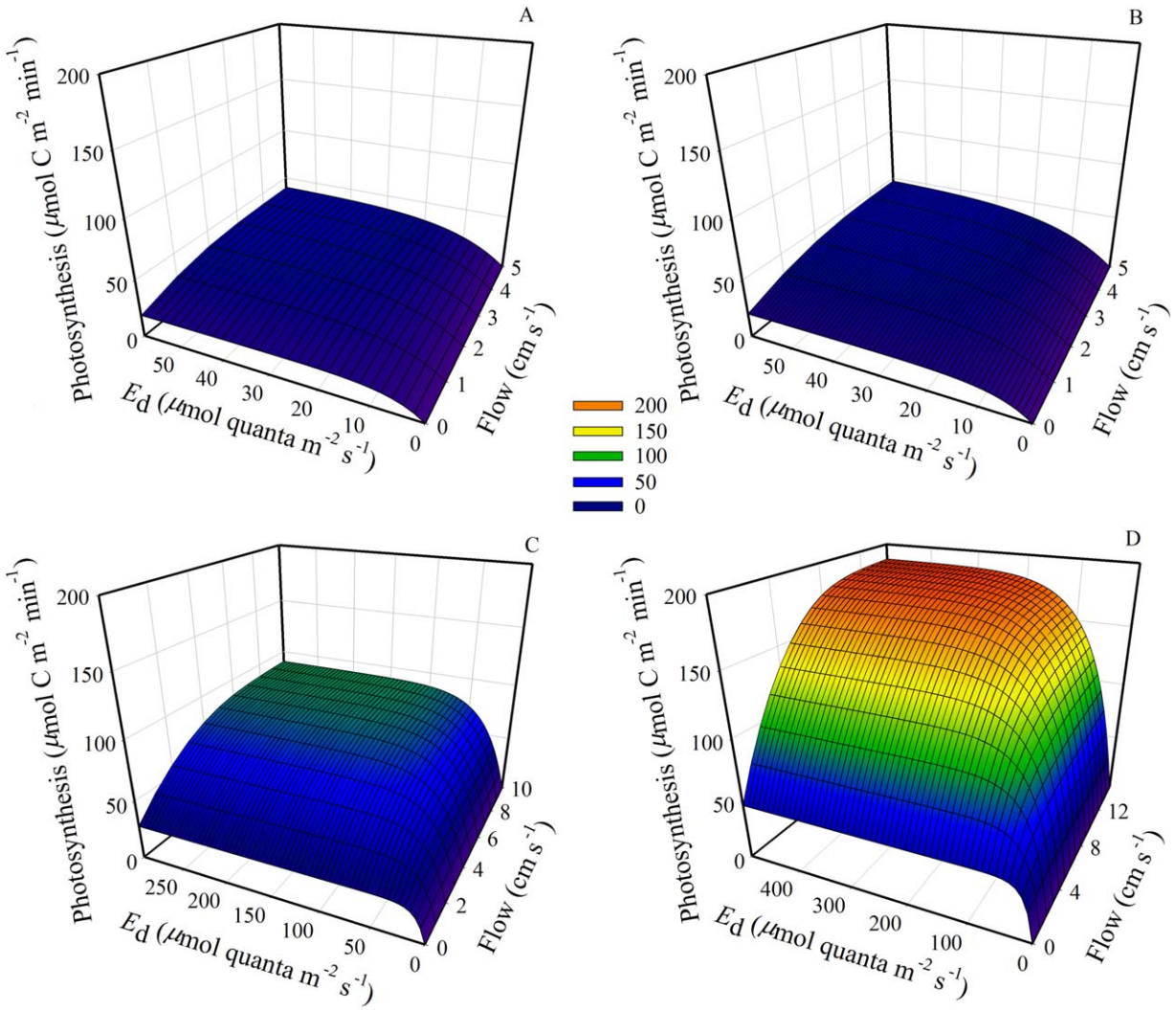

Fig. 4. Three-dimensional representations of the combined influence of irradiance and flow on photosynthesis at four [DIC] derived from Eq. 1. Cool colors indicate low photosynthetic rates; warm colors represent high photosynthetic rates. (A) [DIC] = 1058 μM, [$CO_{2(aq)}$] = 12 μM. (B) [DIC] = 1140 μM, [$CO_{2(aq)}$] = 43 μM. (C) [DIC] = 1565 μM, [$CO_{2(aq)}$] = 445 μM. (D) [DIC] = 2534 μM, [$CO_{2(aq)}$] = 1411 μM]. [Color figure can be viewed in the online issue, which is available at wileyonlinelibrary.com.]

Modeling light saturated $\delta^{13}C$

P_E/P_m increased non-linearly as a function of [DIC] and flow (Fig. 5A) and ranged from 0.11 ([DIC] = 1059 μmol L^{-1}; $u = 0$ cm s^{-1}) to 0.90 ([DIC] = 2533 μmol L^{-1}; $u = 20$ cm s^{-1}). The low value served as the endmember where extreme carbon-limitation prevented isotope discrimination and the high value represented carbon-replete conditions that permitted full isotopic discrimination by RUBISCO. Using the single linear relationship between P_E/P_m and the theoretical photosynthetic ^{13}C fractionation of $-28‰$ relative to the source DIC for RUBISCO, stable carbon isotope signatures were predicted across a range of environmental conditions (Fig. 5B). Along with alkalinity, [DIC] controlled the relative distributions of $CO_{2(aq)}$ and HCO_3^- in seawater, which have

Table 4. Irradiance (E_k) required to achieve light-saturated photosynthesis ($P = P_E$, Eq. 1) for a range of DIC concentrations in still water (0 cm s^{-1}) and flow-saturated conditions (15 cm s^{-1}).

	E_k (μmol quanta m^{-2} s^{-1})	
[DIC] (μmol L^{-1})	Flow 0 cm s^{-1}	Flow 15 cm s^{-1}
1058	6.1	13.0
1140	6.5	15.3
1565	9.0	29.1
2534	14.6	60.3

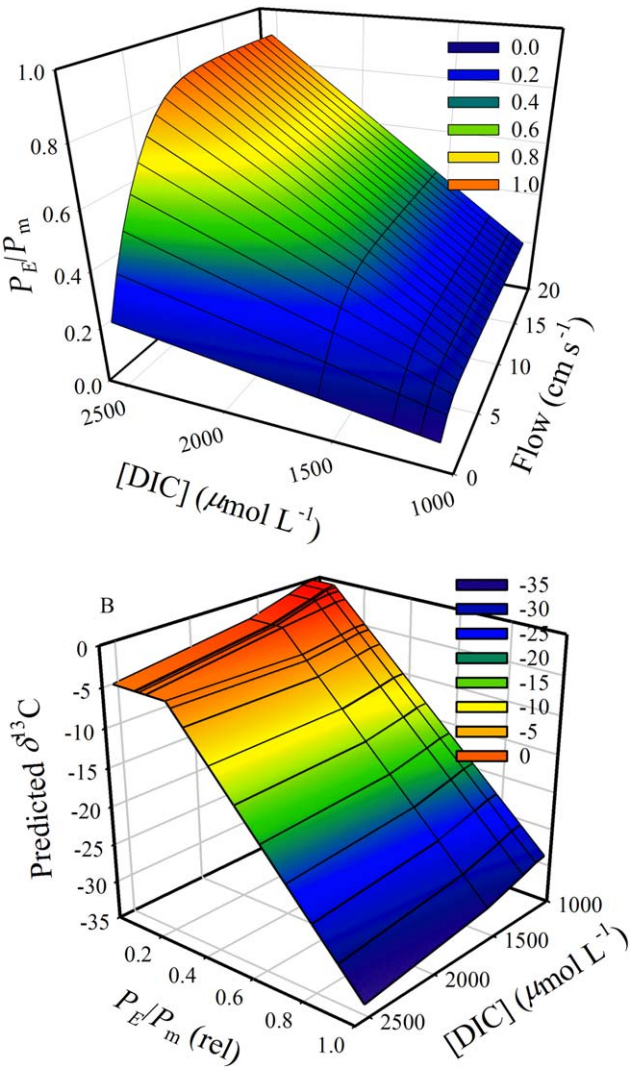

Fig. 5. (A) The combined effects of flow and [DIC] on P_E/P_m. P_E/P_m represents the degree to which light-saturated photosynthesis (P_E) is saturated with respect to flow and [DIC]. When $P_E/P_m = 1$, the supply of DIC exceeds demand and isotopic discrimination is controlled purely by RUBISCO. (B) The effect of P_E/P_m on $\delta^{13}C$ based on a simple linear mixing model based on [DIC] and the effect of pH on the speciation of $[CO_{2(aq)}]$ and $[HCO_3^-]$. [Color figure can be viewed in the online issue, which is available at wileyonlinelibrary.com.]

characteristically different isotopic signatures (−9‰ and 0‰, respectively; Kroopnick 1985). Although there were large gradients in the proportions of $[HCO_3^-]$ and $[CO_{2(aq)}]$ across the pH gradient (Fig. 2C), the effect of DIC source only approached the −9‰ difference in $\delta^{13}C$ between HCO_3^- and $CO_{2(aq)}$ where $P_E/P_m < 0.4$. The predicted $\delta^{13}C$ decreased as the photosynthesis became both carbon- and flow-replete (increasing P_E/P_m), with the relatively small differences in $\delta^{13}C$ across the pH gradient representing the increasing impact of RUBISCO discrimination regardless of the DIC source.

In general, [DIC] and flow combined to predict light-saturated values of $\delta^{13}C$ between −25‰ and −1‰ (Fig. 6). Light-saturated $\delta^{13}C$ decreased non-linearly as flow increased, becoming insensitive to flow above 3 cm s^{-1}. However, $\delta^{13}C$ decreased linearly with [DIC], and the slope of that relationship increased with flow. The steepest gradients in predicted $\delta^{13}C$ signatures occurred between carbon-limited (~ 1000 μmol L^{-1}) and carbon-replete (~ 2500 μmol L^{-1}) DIC concentrations under high flow conditions ($u > 2$ cm s^{-1}).

Photosynthesis vs. $CO_{2(aq)} + HCO_3^-$ data from Invers et al. (2001) provide a useful test of model predictions of $\delta^{13}C$ from P_E/P_m for four ecologically important seagrasses, revealing differences in carbon species utilization. Rates of light saturated photosynthesis re-scaled to P_m corresponded well to modeled values of P_E/P_m (Fig. 7, filled circles). Using the kinetic parameters provided in Table 4 of Invers et al. (2001), the model estimated the contribution of $[HCO_3^-]$, and by difference the contribution of $[CO_{2(aq)}]$ to P_E/P_m (Fig. 7, dotted lines and dash-dot-dot lines, respectively). High concentrations of HCO_3^- (~ 2000 μmol L^{-1}) relative to K_s (260–800 μmol L^{-1}) produced a near constant estimate of P_E/P_m based on $[HCO_3^-]$ for each species across most of the $CO_{2(aq)}$ range and declined at the highest value of $CO_{2(aq)}$ where $[HCO_3^-]$ dropped to 1400 μmol L^{-1}. However, P_E/P_m derived from HCO_3^- was much lower for *Z. marina* and *Phyllospadix torreyi*, and photosynthesis was more effectively stimulated by $CO_{2(aq)}$, than for *Posidonia oceanica* and *Cymodocea nodosa*. Values of light-saturated $\delta^{13}C$ derived from model predictions of P_E/P_m declined for all species as the fraction of photosynthesis derived from $CO_{2(aq)}$ increased

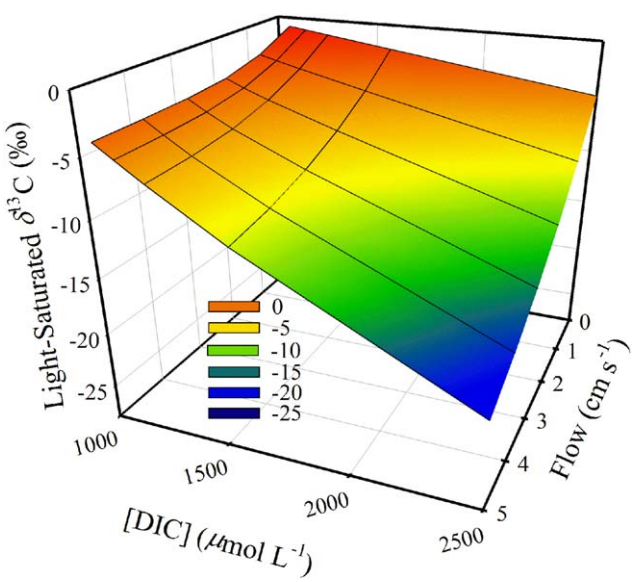

Fig. 6. Effects of flow and [DIC] on the $\delta^{13}C$ signature for light-saturated photosynthesis, derived from the average linear relationship between P_E/P_m and predicted $\delta^{13}C$ signature illustrated in Fig. 5B. [Color figure can be viewed in the online issue, which is available at wileyonlinelibrary.com.]

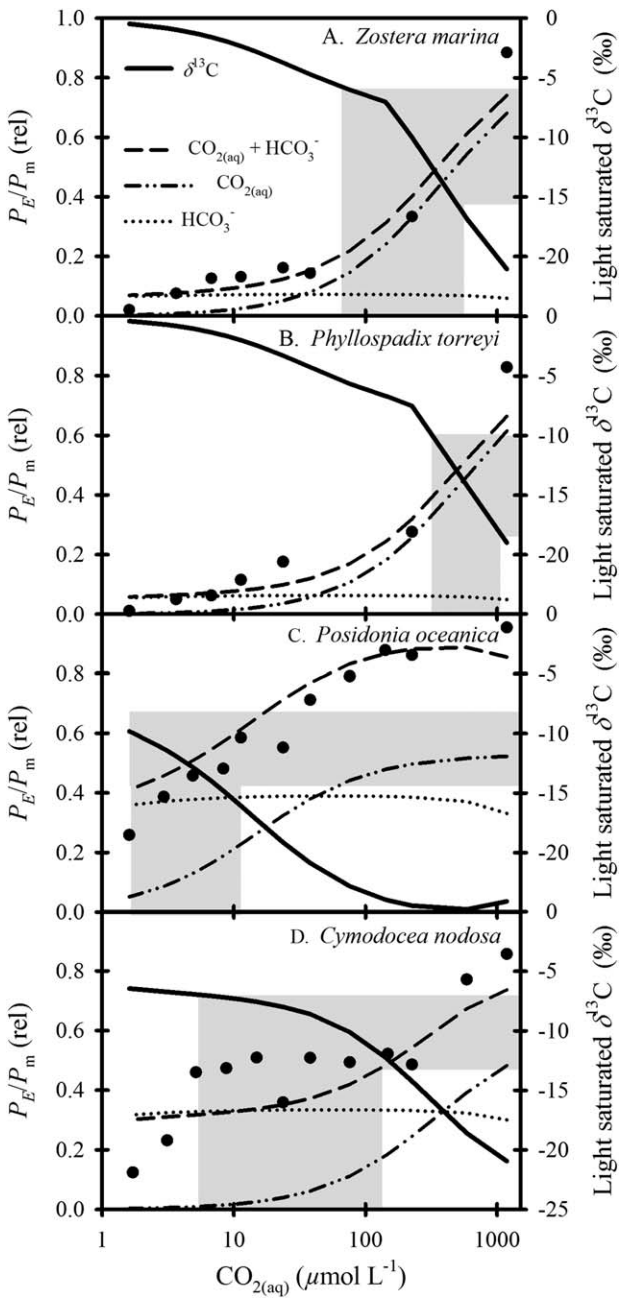

Fig. 7. Modeled effects of $CO_{2(aq)}$ on P_E/P_m and light-saturated $\delta^{13}C$ for (A) *Zostera marina*, (B) *Phyllospadix torreyi*, (C) *Posidonia oceanica* and (D) *Cymodocea nodosa*. Original data (filled circles) were derived from Invers et al. (2001). Broken lines indicate relative contributions of HCO_3^-, $CO_{2(aq)}$ and $CO_{2(aq)} + HCO_3^-$ to P_E/P_m. Solid black line indicates the corresponding value of $\delta^{13}C$ predicted by the model. Shaded areas indicate the $CO_{2(aq)}$ concentrations required to generate the range of $\delta^{13}C$ values for each genus reported by Hemminga and Mateo (1996).

(Fig. 7, solid lines). The range of $\delta^{13}C$ predicted for the entire $CO_{2(aq)}$ series was greatest for *Z. marina* (21‰), followed by *P. torreyi* (19‰), *P. oceanica* (15‰), and *C. nodosa* (14‰). Constraining model predictions of $\delta^{13}C$ to the range of values for these genera published by Hemminga and Mateo (1996; their Table 1) suggests that these species inhabit different $CO_{2(aq)}$ environments despite the overlapping values of $\delta^{13}C$ (Fig. 7 shaded regions).

Discussion

The modeling analysis undertaken here generated a quantitative understanding of the simultaneous regulation of eelgrass photosynthesis by light availability, flow, and [DIC] and informed predictions of leaf $\delta^{13}C$. Although light is the primary source of photosynthetic energy, photosynthesis is also controlled by the combined effects of [DIC] in the bulk fluid and the influence of flow on DIC transport to the leaf surface. When photosynthesis is not limited by delivery of DIC to the reaction site (i.e., $P < P_E$ or $P = P_m$), the isotope discrimination property of RUBISCO (about −28‰ relative to the source DIC) determines $\delta^{13}C$. However, when photosynthesis is carbon limited (i.e., $P = P_E$ and $P_E < P_m$), $\delta^{13}C$ depends on the ratio of P_E/P_m, which allows environmental parameters such as flow and [DIC] to affect carbon isotope fractionation. Consequently, the estimates of $\delta^{13}C$ provided here based on P_E/P_m represent an upper (heavy) bound for isotopic signatures, and true values will be more negative to the extent that light limitation of photosynthesis resulting from water depth/transparency, canopy architecture and meadow density, allows isotopic discrimination to be controlled by RUBISCO rather than by DIC supply.

Although P_m was considered a physiological constant in this model, the carbon fixation activity of RUBISCO is also affected by temperature. In the absence of carbon limitation, however, temperature effects on enzyme activity are confounded by compensating effects on CO_2 solubility and diffusion. Thus, the influence of temperature on carbon isotope discrimination appears to be considerably weaker than the effect of [DIC] or light, and may be difficult to observe in nature (Carvalho et al. 2010). For example, most of the seasonal variation in leaf $\delta^{13}C$ (~ 1.4‰) for *Thalassia testudinum* growing in Florida Bay and the Bahamas can be attributed to variations in light availability, even though temperature ranges seasonally from 16°C to 29°C (Hu et al. 2012). P_m can also be affected by numerous RUBISCO activation factors, including molecular chaperones and various anionic effectors including sulfate, orthophosphate, phosphorylated sugars and/or NADPH involved in sucrose formation that operate independently of the CO_2 supply (McCurry et al. 1981; Marcus and Gurevitz 2000). However, eelgrass is not known to exhibit circadian patterns in sucrose formation capacity and appears to possess sufficient sucrose formation activity to prevent phosphate limitation or starch accumulation in the chloroplast that might de-activate RUBISCO, even when photosynthesis rates are stimulated by high [$CO_{2(aq)}$] (Zimmerman et al. 1995).

The permeability term (U_p) provided a mechanistic link between the effects of flow and [DIC] on light-saturated photosynthesis and $\delta^{13}C$. Although previously defined by Smith and Walker (1980) as the concentration-dependent permeability of the unstirred layer through which the substrate must diffuse to reach the reaction site, our model re-defined U_p as a function of flow (Eq. 4) while retaining the original, concentration-dependent permeability in still water as U_{p0}. The broader definition of U_p made it an aggregate product of flow and [DIC], and permitted the model to characterize DIC transport to the reaction site under a broad range of [DIC] and flow conditions. This approach also produced large uncertainties around predictions of U_p from Eq. 2, a function of the insensitive nature of complex non-linear models to certain parameters, particularly when they are not completely independent (Zimmerman et al. 1987), as is the case for U_p and K_s. In this case, it appeared that variations in U_p had little effect on the relationship between P_F and concentration. Despite high variability, mean U_p values from Eq. 2 reliably predicted photosynthesis, but also reinforce the need for deeper insight into the mechanisms by which flow and [DIC] control U_p and K_s.

As defined in this model, K_s represents an operational half-saturation constant integrating DIC transport between the bulk fluid and the reaction site in the chloroplast stroma with the substrate binding kinetics for RUBISCO. Consequently, the different values of K_s obtained for $CO_{2(aq)}$ and DIC (mostly HCO_3^- for pH 6–9) reflect differences in the transport capacity for $CO_{2(aq)}$ and HCO_3^-. Although useful in the context of this model, these values are higher than the true dissociation constant (K_m) for RUBISCO that depends only on substrate binding properties of the enzyme with respect to the local concentration of CO_2 in the chloroplast stroma.

Seagrasses utilize HCO_3^- to varying degrees in support of photosynthesis, and it may be the primary source of DIC for oceanic environments where pH and salinity are high and relatively stable (Prins and Elzenga 1989; Hellblom et al. 2001). However, only $CO_{2(aq)}$ has been demonstrated to stimulate P_E to P_m, indicating that many seagrasses, including oceanic species, are less efficient at exploiting HCO_3^- than other primary hydrophytes that do not respond to elevated [$CO_{2(aq)}$] (Raven et al. 1985). Experiments conducted here using AZ suggested limited use of CA by eelgrass from the Goodwin Islands NERR to facilitate DIC uptake via conversion of HCO_3^- to $CO_{2(aq)}$ under ambient $CO_{2(aq)}$ conditions, which differs from studies conducted on other populations of eelgrass that found a 20–50% depression in photosynthesis by inhibiting external CA (Hellblom et al. 2001). Although HCO_3^- uptake via dehydration and proton pumping (Hellblom et al. 2001; Hellblom and Axelsson 2003; Beer et al. 2006) or anion exchange cannot be ruled out as a possible mechanism for exploiting HCO_3^- in support of photosynthesis, our experimental findings suggest that Goodwin Islands eelgrass photosynthesis were substrate limited by [$CO_{2(aq)}$], and are consistent with previous observations of the profound positive effects of [$CO_{2(aq)}$] on photosynthetic rates of many seagrasses (Invers et al. 2001; Jiang et al. 2010; Campbell and Fourqurean 2013), in addition to eelgrass (Zimmerman et al. 1995; Palacios and Zimmerman 2007). Thus, the parameterization of U_p and P_F for eelgrass was more responsive to [$CO_{2(aq)}$] than [DIC], which is dominated by [HCO_3^-] for most of the pH 6–8 range. However, the parameterization employed here can also accommodate differences in HCO_3^- utilization among species.

When applied to the four seagrass species examined by Invers et al. (2001), the model predicted different $CO_{2(aq)}$ environments corresponding to the range of published $\delta^{13}C$ values (Hemminga and Mateo 1996, their Table 1) that could be attributed to differences in $CO_{2(aq)}$ and HCO_3^- utilization. The weak capacity for HCO_3^- utilization relative to P_m exhibited by eelgrass and *P. torreyi* suggests that these species rely primarily on $CO_{2(aq)}$ for photosynthetic carbon. The published range of $\delta^{13}C$ values (−6‰ to −19‰) for these two genera correspond to modeled $CO_{2(aq)}$ concentrations between 75 μM and 500 μM. Although these conditions are well above air-saturation, the wide salinity tolerance of *Zostera* allows it to occupy shallow polyhaline regions of many temperate estuaries characterized by high variability in pH, including values as low as 7, resulting from terrestrial runoff and ecosystem metabolism that involves high rates of respiration, periodically elevating [$CO_{2(aq)}$] well above air saturation and depressing pH values close to 7 (Duarte et al. 2013). These relationships also imply that $\delta^{13}C$ of *Zostera* should increase along estuarine gradients in proportion to the degree of oceanic influences that serve to stabilize salinity and pH at relatively high values, consistent with recently published observations (Ruesink et al. 2015). Additionally, water column optical properties in coastal regions show considerable temporal-spatial variation (Zimmerman et al. 1994; McPherson et al. 2011), and will alter the fraction of the day that plants experience light-saturated conditions, biasing leaf $\delta^{13}C$ to values lighter than predicted by P_E/P_m.

Phyllospadix torreyi is unique among seagrasses in colonizing intertidal regions of wave-swept rocky shores along the open coast of the eastern Pacific. The shallow colonization depths, near-constant water motion, frequent exposure to energetic breaking waves and sea foam, plus frequent exposure to air at low tide suggest that the relatively light $\delta^{13}C$ values for this species may result from uptake of a large fraction of its photosynthetic carbon directly from the air, which, because of higher diffusion rates, is operationally consistent with the very high concentrations of $CO_{2(aq)}$ required by the model to generate published $\delta^{13}C$ values. Greater capacity for HCO_3^- utilization by *Posidonia* spp. and *Cymodocea* spp. required lower [$CO_{2(aq)}$] to match published values of $\delta^{13}C$, consistent with the subtidal distribution of these species in the salty, warm, oligotrophic waters of the Mediterranean, where they experience lower volumes of

terrestrial runoff, less variability in water column metabolic activity, and more stable pH and [DIC] conditions than *Zostera* spp. and *Phyllospadix* spp.

Differences in utilization of inorganic carbon species can influence the $\delta^{13}C$ signatures of marine autotrophs (Maberly et al. 1992; Raven et al. 2002) and may explain some of the species-level differences in $\delta^{13}C$ among seagrasses as described above. Some of the CO_2 generated by respiration is captured by the lacunae and may provide an additional source of CO_2 to RUBISCO (Grice et al. 1996). However, split-chamber incubations suggest that the lacunae of eelgrass and turtlegrass capture about 6% of the photosynthetic O_2 generated by the leaves (Bodensteiner 2006). Assuming a similar amount of the respiratory CO_2 is internally recycled, a P_E/R of 5 would generate only 1.2% of the CO_2 required for photosynthesis. Furthermore, $\delta^{13}C$ of the respired CO_2 is likely to be very similar to that of the tissue from which it was derived. Consequently, the impact of internal CO_2 recycling on $\delta^{13}C$ is likely to be minimal.

Our model showed a significant influence of the carbon source [$CO_{2(aq)}$ vs. HCO_3^-] on $\delta^{13}C$ signatures only when photosynthesis (P_E) was light-saturated but carbon-limited (i.e., $P = P_E = P_F < P_m$), thereby restricting isotopic discrimination by RUBISCO. This reinforces the impact that environmental conditions, such as light availability and flow (Koch 2001) can have on the isotopic signature of carbon-limited seagrasses (Durako and Hall 1992; Hu et al. 2012; Kim et al. 2014), and points the way for generalizing this model to other marine autotrophs that employ a wide range of CCMs and inorganic carbon utilization strategies. Seagrass $\delta^{13}C$ should become increasingly negative along DIC gradients (e.g., estuarine environments) and where rising [$CO_{2(aq)}$] increases P_E/P_m and reduces the fraction of photosynthetic DIC derived from HCO_3^-. However, as P_E approaches P_m, differences in $\delta^{13}C$ resulting from $CO_{2(aq)}$ vs. HCO_3^- utilization become less influential because RUBISCO is increasingly able to discriminate against $^{13}CO_2$. Consequently, this model suggests that there should be little impact of ocean acidification on $\delta^{13}C$ of macroalgae and phytoplankton in which $P_E \cong P_m$ because efficient HCO_3^- utilization increases the importance of isotopic discrimination by RUBISCO in determining $\delta^{13}C$.

Temporal shifts in $\delta^{13}C$ signature within a population (or differences among populations) may point toward specific responses to environmental conditions resulting from changes in light availability (i.e., turbidity), the supply of inorganic carbon (e.g., along estuarine gradients, ocean acidification), and flow conditions (Ruesink et al. 2015). Although the flexible, strap-like leaves of eelgrass become physiologically insensitive to flow-dependent boundary layer effects at relatively low velocities, similar to many marine macrophytes (Koehl and Alberte 1988), P_m cannot be achieved simply by increasing flow at present-day values of oceanic [DIC]. However, flow can affect $\delta^{13}C$ by regulating mass transport of DIC to seagrass leaves in dense meadows when canopy drag increases the boundary layer thickness around the leaves and photosynthesis depletes DIC from the water column (Koch 2001; McKone 2009). Thus, $\delta^{13}C$ of seagrass from high flow areas should be more responsive to changes in [DIC], and particularly [$CO_{2(aq)}$] because of steep gradients between flow-saturated and flow-limited photosynthesis at high [$CO_{2(aq)}$]. Deeper insight into the mechanisms by which flow and [DIC] control U_p may lead to a better understanding of the factors determining the empirical K_s, which is a product of the boundary layer and leaf structure characteristics that resist DIC transport, as well as the native K_m for purified RUBISCO.

High light environments that cause photosynthesis to be carbon-limited most of the day decrease isotopic discrimination in seagrasses and result in heavier $\delta^{13}C$ signatures (Hu et al. 2012). Reducing the substrate limitation of RUBISCO by, e.g., decreasing light or increasing CO_2 availability, increases discrimination against $^{13}CO_2$, producing isotopically lighter $\delta^{13}C$ signatures. This model provides a path for calculating $\delta^{13}C$ in nature from knowledge of the fraction of the day photosynthesis is light-saturated (i.e., $P = P_E$) by quantifying complex interaction between [DIC], flow, and permeability on $\delta^{13}C$ signature under light saturation. However, it should be noted that the low saturating irradiances (E_k) reported here were obtained from measurements on individual leaves uniformly illuminated by a normal (i.e., perpendicular) downwelling irradiance field that maximized light absorption. These E_k values, although consistent with similar measures performed under laboratory conditions, are lower than the ecological E_k for intact submerged plant canopies that are affected by leaf orientation and canopy density that control self-shading (Zimmerman 2003). Nonetheless, the functional relationships developed here quantifying the effects of light, flow and [DIC] on stable carbon isotope signatures at the level of the individual leaf are readily extended to submerged plant canopies using spatially resolved bio-optical models capable of estimating daily integrated photosynthesis of seagrass meadows in the field as functions of canopy architecture that depend on shoot size, density, leaf orientation and flow, as well as submarine irradiance controlled by water column transparency, depth, and time (Zimmerman 2003; Hedley and Enríquez 2010). In addition to providing a stronger mechanistic basis for the frequently observed correlations between carbon isotope signatures and environment, the incorporation of these relations into radiative transfer models provides a vehicle to generalize the relationship between leaf $\delta^{13}C$ and light/water quality, DIC availability, temperature, and even epiphyte load. Understanding environmental control of carbon uptake in seagrasses will become increasingly important for predicting the responses of these important ecosystem engineers to anthropogenic climate change, ranging from local processes affecting eutrophication, light availability and flow to global impacts of climate warming and ocean acidification.

References

Beer, S., L. Axelson, and M. Bjork. 2006. Modes of photosynthetic bicarbonate utilisation in seagrasses, and their possible roles in adaptations to specific habitats. *In* M. C. Gambi, J. A. Borg, M. C. Buia, G. Di Carlo, C. Pergent-Martini, G. Pergent, G. Procaccini, [eds.], Mediterranean Seagrass Workshop.

Bjork, M., A. Weil, S. Semesi, and S. Beer. 1997. Photosynthetic utilisation of inorganic carbon by seagrasses from Zanzibab, East Africa. Mar. Biol. **129**: 363–366. doi:10.1007/s002270050176

Bodensteiner, L. 2006. The impact of light availability on benthic oxygen release by the seagrasses *Thalassia testudinum* (Banks ex König) and *Zostera marina* (L.). MS Thesis. San Jose State Univ.

Campbell, J. E., and J. W. Fourqurean. 2009. Interspecific variation in the elemental and stable isotope content of seagrasses in South Florida. Mar. Ecol. Prog. Ser. **387**: 109–123. doi:10.3354/meps08093

Carvalho de Carvalho, M., K. Hayashizaki, and H. Ogawa. 2010. Temperature effect on carbon isotopic discrimination by *Undaria pinnatifida* (Phaeophyta) in a closed experimental system. J. Phycol. **46**: 1180–1186. doi:10.1111/j.1529-8817.2010.00895.x

Cooper, L. W., and M. J. Deniro. 1989. Stable carbon isotope variability in the seagrasses *Posidonia oceanica*: Evidence for light intensity effects. Mar. Ecol. Prog. Ser. **50**: 225–229. doi:10.3354/meps050225

Denny, M. W. 1993. Air and water. Princeton Univ. Press.

Duarte, C. 2002. The future of seagrass meadows. Environ. Conserv. **29**: 192–206. doi:10.1017/S0376892902000127

Duarte, C., and others. 2013. Is ocean acidification an open-ocean syndrome? Understanding the drivers and impacts of pH variability in coastal ecosystems. Estuaries Coasts **36**: 221–236. doi:10.1007/s12237-013-9594-3

Durako, M. J., and M. O. Hall. 1992. Effects of light on the stable carbon isotope composition of the seagrass *Thalassia testudinum*. Mar. Ecol. Prog. Ser. **86**: 99–101. doi:10.3354/meps086099

Falkowski, P. G., and J. A. Raven. 2007. Aquatic photosynthesis, 2nd ed. Princeton Univ. Press.

Farquhar, G. D., J. R. Ehleringer, and K. T. Hubick. 1989. Carbon isotope discrimination and photosynthesis. Annu. Rev. Plant Physiol. Plant Mol. Biol. **40**: 503–537. doi:10.1146/annurev.pp.40.060189.002443

Fourqurean, J., S. Escorcia, W. Anderson, and J. Zieman. 2005. Spatial and seasonal variability in elemental content, δ^{13}C and δ^{15}N of *Thalassia testuninum* from South Florida and its implications for ecosystem studies. Estuaries Coasts **28**: 447–461. doi:10.1007/BF02693926

France, R. L. 1995. Carbon-13 enrichment in benthic compared to planktonic algae: Foodweb implications. Mar. Ecol. Prog. Ser. **124**: 307–312. Doi:10.3354/meps124307

Gieskes, J. M., and W. C. Rogers. 1973. Alkalinity determination in interstitial waters of marine sediments. J. Sediment Res. **43**: 272–277. doi:10.1306/74D72743-2B21-11D7-8648000102C1865D

Grice, A. M., N. R. Loneragan, and W. C. Dennison. 1996. Light intensity and the interactions between physiology, morphology and stable isotope ratios in five species of seagrass. J. Exp. Mar. Biol. Ecol. **195**: 91–110. doi:10.1016/0022-0981(95)00096-8

Hedley, J., and S. Enríquez. 2010. Optical properties of canopies of the tropical seagrass *Thalassia testudinum* estimated by a 3-dimensional radiative transfer model. Limnol. Oceanogr. **55**: 1537–1550. doi:10.4319/lo.2010.55.4.1537

Hellblom, F., and L. Axelsson. 2003. External HCO_3^- dehydration maintained by acid zones in the plasma membrane is an important component of the photosynthetic carbon uptake in *Ruppia cirrhosa*. Photosynth. Res. **77**: 173–181. doi:10.1023/A:1025809415048

Hellblom, F., S. Beer, M. Bjork, and L. Axelsson. 2001. A buffer-sensitive inorganic carbon utilization system in *Zostera marina*. Aquat. Bot. **69**: 55–62. doi:10.1016/S0304-3770(00)00132-7

Hellblom, F., and M. Björk. 1999. Photosynthetic responses in *Zostera marina* to decreasing salinity, inorganic carbon content and osmolality. Aquat. Bot. **65**: 97–104. doi:10.1016/S0304-3770(99)00034-0

Hemminga, M. A., and M. A. Mateo. 1996. Stable carbon isotopes in seagrasses: Variability in ratios and use in ecological studies. Mar. Ecol. Prog. Ser. **140**: 285–298. doi:10.3354/meps140285

Hill, R., and C. P. Whittingham. 1955. Photosynthesis. Methuen.

Hu, X., D. J. Burdige, and R. C. Zimmerman. 2012. δ^{13}C is a signature of light availability and photosynthesis in seagrass. Limnol. Oceanogr. **57**: 441–448. doi:10.4319/lo.2012.57.2.0441

Hurd, C. L. 2000. Water motion, marine macroalgae physiology, and production. J. Phycol. **36**: 453–472. doi:10.1046/j.1529-8817.2000.99139.x

Invers, O., M. Pérez, and J. Romero. 1999. Bicarbonate utilization in seagrass photosynthesis: Role of carbonic anhydrase in *Posidonia oceanica* (L.) Delile and *Cymodocea nodosa* (Ucria) Ascherson. J. Exp. Mar. Biol. Ecol. **235**: 125–133. doi:10.1016/S0022-0981(98)00172-5

Invers, O., R. C. Zimmerman, R. S. Alberte, M. Perez, and J. Romero. 2001. Inorganic carbon sources for seagrass photosynthesis: An experimental evaluation of bicarbonate use in species inhabiting temperate waters. J. Exp. Mar. Biol. Ecol. **265**: 203–217. doi:10.1016/S0022-0981(01)00332-X

James, P. L., and A. W. D. Larkum. 1996. Photosynthetic inorganic carbon acquisition of *Posidonia australis*. Aquat. Bot. **55**: 149–157. doi:10.1016/S0304-3770(96)01074-1

Jiang, Z. J., X.-P. Huang, and J.-P. Zhang. 2010. Effects of CO_2 enrichment on photosynthesis, growth, and biochemical composition of seagrass *Thalassia hemprichii*

(Ehrenb.) Aschers. J. Integr. Plant Biol. **52**: 904–913. doi:10.1111/j.1744-7909.2010.00991.x

Kim, M.-S., S.-M. Lee, H.-J. Kim, S.-Y. Lee, S.-H. Yoon, and K.-H. Shin. 2014. Carbon stable isotope ratios of new leaves of *Zostera marina* in the mid-latitude region: Implications of seasonal variation in productivity. J. Exp. Mar. Biol. Ecol. **461**: 286–296. doi:10.1016/j.jembe.2014.08.015

Koch, E. 2001. Beyond light: Physical, geological, and geochemical parameters as possible submersed aquatic vegetation habitat requirements. Estuaries **24**: 1–17. doi:10.2307/1352808

Koehl, M. A. R., and R. S. Alberte. 1988. Flow, flapping and photosynthesis of *Nereocystis lutkeana*: A functional comparison of undulate and flat blade morphologies. Mar. Biol. **99**: 435–444. doi:10.1007/BF02112137

Kroopnick, P. M. 1985. The distribution of ^{13}C of ΣCO_2 in the world oceans. Deep-Sea Res. Part A. Oceanogr. Res. Pap. **32**: 57–84. doi:10.1016/0198-0149(85)90017-2

Lewis, D. E., and D. W. R. Wallace. 2006. MS. Program Developed for CO2 system calculations. Oak Ridge National Laboratory.

Maberly, S. C., J. A. Raven, and A. M. Johnston. 1992. Discrimination between ^{12}C and ^{13}C by marine plants. Oecologia **91**: 481–492. doi:10.1007/BF00650320

Madsen, T. V., and K. Sand-Jensen. 1991. Photosynthetic carbon assimilation in aquatic macrophytes. Aquat. Bot. **41**: 5–40. doi:10.1016/0304-3770(91)90037-6

Marcus, Y., and M. Gurevitz. 2000. Activation of cyanobacterial RuBP-carboxylase/oxygenase is facilitated by inorganic phosphate via two independent pathways. Eur. J. Biochem. **267**: 5995–6003. doi:10.1046/j.1432-1327.2000.01674.x

McCurry, S., J. Pierce, N. Tolbert, and W. Orme-Johnson. 1981. On the mechanism of the effector mediated activation of ribulose bis-phosphate carboxylase-oxygenase. J. Biol. Chem. **256**: 6623–6628.

McKone, K. L. 2009. Light available to the seagrass *Zostera marina* when exposed to currents and waves. MS Thesis. Univ. of Maryland, College Park.

McPherson, M. L., V. J. Hill, R. C. Zimmerman, and H. M. Dierssen. 2011. The optical properties of Greater Florida Bay: Implications on seagrass abundance. Estuaries Coasts **34**: 1150–1160. doi:10.1007/s12237-011-9411-9

Mercado, J. M., F. X. Niell, J. Silva, and R. Santos. 2003. Use of light and inorganic carbon aquition by two morphotypes of *Zostera noltii* Hornem. J. Exp. Mar. Biol. Ecol. **297**: 71–84. doi:10.1016/S0022-0981(03)00368-X

O'Leary, M. H. 1981. Carbon isotope fractionation in plants. Phytochemistry **20**: 553–567. doi:10.1016/0031-9422(81)85134-5

Orth, R. J., and others. 2006. A global crisis for seagrass ecosystems. Biosci. Mag. **56**: 987–995. doi:10.1641/0006-3568(2006)56[987:AGCFSE]2.0.CO;2

Palacios, S. L., and R. C. Zimmerman. 2007. Response of eelgrass *Zostera marina* to CO_2 enrichment: Possible impacts of climate change and potential for remediation of coastal habitats. Mar. Ecol. Prog. Ser. **344**: 1–13. doi:10.3354/meps07084

Penhale, P. A. 1977. Macrophyte-epipyte biomass and productivity in an eelgrass (*Zostera marina* L.) community. J. Exp. Mar. Biol. Ecol. **26**: 211–224. doi:10.1016/0022-0981(77)90109-5

Peterson, B. J., and B. Fry. 1987. Stable isotopes in ecosystem studies. Annu. Rev. Ecol. Syst. **18**: 293–320. doi:10.1146/annurev.es.18.110187.001453

Prins, H. B. A., and J. T. M. Elzenga. 1989. Bicarbonate utilization: Function and mechanism. Aquat. Bot. **34**: 59–83. doi:10.1016/0304-3770(89)90050-8

Raven, J. A., B. Osborne, and A. M. Johnston. 1985. Uptake of CO_2 by aquatic vegetation. Plant Cell Environ. **8**: 417–425. doi:10.1111/j.1365-3040.1985.tb01677.x

Raven, J. A., N. A. Walker, A. M. Johnston, L. L. Handley, and J. E. Kubler. 1995. Implications of ^{13}C natural abundance measurements for photosynthetic performance by marine macrophytes in their natural environment. Mar. Ecol. Prog. Ser. **123**: 193–205. doi:10.3354/meps123193

Raven, J. A., and others. 2002. Mechanistic interpretation of carbon isotope discrimination by marine macroalgae and seagrasses. Funct. Plant Biol. **29**: 355–378. doi:10.1071/pp01201

Ruesink, J., S. Yang, and A. Trimble. 2015. Variability in carbon availability and eelgrass (*Zostera marina*) biometrics along an estuarine gradient in Willapa Bay, WA, USA. Estuaries Coasts: 1–10. doi:10.1007/s12237-014-9933-z

Smith, B. N., and S. Epstein. 1971. Two catagories of $^{13}C/^{12}C$ ratios for higher plants. Plant Physiol. **47**: 380–384. doi:10.1104/pp.47.3.380

Smith, F. A., and N. A. Walker. 1980. Photosynthesis by aquatic plants: Effects of unstirred layers in relation to assimilation of CO_2 and HCO_3^- and to carbon isotopic discrimination. New Phycol. **86**: 245–259. doi:10.1111/j.1469-8137.1980.tb00785.x

Webb, W. L., M. Newton, and D. Starr. 1974. Carbon dioxide exchange of *Alnus rubra*. Oecologia **17**: 281–291. doi:10.1007/BF00345747

Zeebe, R. E., and D. A. Wolf-Gladrow. 2001. CO_2 in seawater: Equilibrium, kinetics, isotopes, 1st ed. Elsevier.

Zhang, J., P. D. Quay, and D. O. Wilbur. 1995. Carbon isotope fractionation during gas-water exhange and dissolution of CO_2. Geochim. Cosmochim. Acta **59**: 107–114. doi:10.1016/0016-7037(95)91550-D

Zimmerman, R., A. Cabello-Pasini, and R. Alberte. 1994. Modeling daily production of aquatic macrophytes from irradiance measurements: A comparative analysis. Mar. Ecol. Prog. Ser. **114**: 185–196. doi:10.3354/meps114185

Zimmerman, R., D. Kohrs, D. L. Steller, and R. Alberte. 1995. Carbon partitioning in eelgrass. Regulation by photosynthesis and the response to daily light-dark cycles. Plant Physiol. **108**: 1665–1671. doi:10.1104/pp.108.4.1665

Zimmerman, R. C. 2003. A biooptical model of irrandiance distribution and photosynthesis in seagrass canopies. Limnol. Oceanogr. **48**: 568–585. doi:10.4319/lo.2003.48.1_part_2.0568

Zimmerman, R. C., D. G. Kohrs, D. L. Steller, and R. S. Alberte. 1997. Impacts of CO_2 enrichment on productivity and light requirements of Eelgrass. Plant Physiol. **115**: 599–607.

Zimmerman, R. C., J. B. Soohoo, J. N. Kremer, and D. Z. D'Argenio. 1987. Evaluation of variance approximation techniques for non-linear photosynthesis-irradiance models. Mar. Biol. **95**: 209–215. doi:10.1007/BF00409007

Acknowledgments

Many thanks to David Ruble, Billur Celebi, Malee Jinuntuya, and Alexander Bochdansky for assistance in the field and lab, and to Alexander Bochdansky, David Burdige, Malcom Scully and Anthony Larkum for critical comments and discussions that improved the quality of this effort. Aeronautical honeycomb material used to create a laminar flow environment in the flume was donated by Plascore Inc. (www.plascore.com). Financial support was provided by the National Science Foundation (OCE 1061823), National Oceanic and Atmospheric Administration Virginia Sea Grant (NA10OAR4170085), and the Department of Ocean, Earth & Atmospheric Sciences, Old Dominion University (www.odu.edu/oeas). This work was completed in partial fulfillment of the requirements for the Masters of Science degree (Ocean and Earth Sciences) at ODU (M. McPherson).

Submitted 13 October 2014
Revised 23 March 2015; 15 June 2015
Accepted 17 June 2015

Associate editor: Anthony Larkum